RESEARCH ARTICLE

Chemical and biological investigations of *Limonium axillare* reveal mechanistic evidence for its antidiabetic activity

Essam Abdel-Sattar[1], **Manal M. Shams**[2], **Marwa M. Abd-Rabo**[ORCID][3], **Nehad Mahmoud**[1], **Engy A. Mahrous**[ORCID][1]*

1 Department of Pharmacognosy, Faculty of Pharmacy, Cairo University, Cairo, Egypt, **2** Department of Medicinal Plants and Natural Products, National Organization of Drug Control and Research, Giza, Egypt, **3** Department of Hormone Evaluation, National Organization of Drug Control and Research, Giza, Egypt

* engy.abdelhamid@pharma.cu.edu.eg

Abstract

Root and bark of *Limonium axillare* (Forssk) Kuntze are used as antidiabetic remedies in parts of East Africa, but this activity has never been fully investigated. To validate its ethnobotanical use, we compared the chemical and pharmacological profiles of the ethanolic extracts of *L. axillare* root (REE) and aerial parts (AEE). Administration of REE (500 mg kg^{-1}) reduced streptozotocin-induced hyperglycemia by 44%, restored serum insulin levels, reestablished Glut2 and Glut4 expression and ameliorated pancreatic tissue damage in diabetic rats. *In vitro* studies revealed a strong radical scavenging effect, α-glucosidase, and α-amylase inhibition activity of REE at IC$_{50}$ at 25.2, 44.8 and 89.1μg/mL, respectively. HPLC analysis identified ten phenolic compounds in REE with umbelliferone as the major constituents at 10 ± 0.081 mg/g of extract. Additionally, six compounds were isolated from REE including, β-sitosterol-3-palmitate, β-sitosterol, myricetin and gallic acids with two new tetrahydrofuran monoterpenes; 2-isopropyl- 3,4,4, trimethyl-tetrahydrofuran (**3**), and 2-isopropyl-4-methyl-tetrahydrofuran-3,4 dicarboxylic acid (**4**), the latter was revealed by molecular docking to be a good ligand to glycerol-3-phosphate dehydrogenase a key enzyme in glycolysis.

Introduction

Diabetes mellitus (DM) is an epidemic metabolic disease characterized by disruption of glycemic homeostasis leading to hyperglycemia, the hallmark of DM. Poorly controlled DM can lead to many complication including micro and macrovascular diseases, neuropathy, diabetic kidney disease and impairment of the immune system. At present, optimized glucose control is recognized as the best approach to reduce the risk of diabetes chronic complications [1, 2]. In areas where access to expensive antidiabetic medication is limited, medicinal plants play an important role in limiting the progress and complications of diseases such as DM [3, 4].

Limonium axillare (Forssk) Kuntze (Family Plumbaginaceae) is a small shrub distributed in desert and coastal land in East Africa especially in Egypt, Eritrea and Sudan [5] and throughout

the Arabian Peninsula where it is known as "Qataf" and "Shelail" [6]. In Eastern Egypt, roots and barks of the plant are used as antidiabetic remedies [7], while in the Arab Peninsula, the decoction of the fresh plant is used to treat depression [8] and as astringent to treat diarrhea [6, 9]. Apart from its ethnobotanical use, previous investigations concluded that the methanolic extract of *L. axillare* has strong antioxidant activity [10]. Also its butanol extract displayed strong antibacterial and antifungal activity when compared to chloramphenicol and nalidixic acid, respectively [11]. The alcohol extract and two phenolic compounds obtained from *L. axillare* leaves have also shown good cytotoxic activity in both *in vitro* and *in vivo* models [12]. Leaves of *L. axillare* were found to contain several flavonoids, namely, apigenin, apiin, luteolin, quercetin, myricetin and kaempferol, in addition to phytosterols, namely, *β*-sitosterol, stigmasterol and *β*- sitosterol glucoside [13]. Meanwhile, the root bark is rich in phenolic acids including gallic, ferulic and isoferulic acid, and a number of coumarins including bergapten, umbelliferone and imperatorin [12].

Since no previous studies were reported to validate the ethnobotanical use of *L. axillare* as an anti-diabetic remedy, this study was designed to chemically investigate the ethanolic extracts obtained from the root system (REE) and the aerial part (AEE) and to correlate their chemical compositions to their antidiabetic activity through *in vivo*, *in vitro* and *in silico* studies. Six compounds were later isolated from the more active root extract resulting in the identification of two novel tetrahydrofuran derivatives.

Material and methods

Chemicals

Streptozotocin (STZ), acarbose, metformin (MF), *p*-nitophenylglucopyranoside, α- glucosidase (*Saccharomyces cerevisiae*), porcine pancreatic α-amylase were purchased from Sigma-Aldrich, St' Louis, MO, USA. Folin-Ciocalteu reagent was purchased from Loba chemie, Mombai, India. External standards for HPLC analysis were either isolated from the plant or supplied by National Organization of Drug Control and Research (NODCAR), Egypt. All solvents were of analytical grade and purchased from Adwic company, Egypt. Acetonitrile and trifluoracetic acid were of HPLC grade and purchased from Sigma-Aldrich (MO, USA). Stationary phases for chromatographic separations were purchased from Merck (Darmstadt, Germany). NMR spectra were acquired using Brucker, Avance, 400 MHz. (MA, USA). MS data were recorded on Shimadzu LCMS-IT-TOF spectrometer (Kyoto, Japan).

Plant material

Flowering aerial parts and roots of *Limonium axillare* (Forssk) Kuntze were collected from the Suez Canal road in January 2017 (29˚ 66' 65'' N, 32˚ 33' 54'' E). The plant was authenticated by Prof. Azza Mohamed Hosney El -Hadidy, Professor of Taxonomy and Flora, Department of Botany, Faculty of Science, Cairo University. A voucher specimen (Voucher no.: 8-3-2018) is deposited in Department of Pharmacognosy, Faculty of Pharmacy, Cairo University.

Preparation of plant extracts

The air-dried powdered root and aerial parts (1.2 kg each) were extracted separately by repeated cold maceration with 70% ethanol (3 x 7 liters) to allow the extraction of phytoconstituents with different solubilities. The extracts were concentrated using vacuum to give 284 g and 154 g of residue of aerial part ethanolic extract (AEE) and root ethanolic extract (REE), respectively. The residue of the two extracts (50 g each) were suspended in water and subjected separately to successive liquid-liquid fractionation with *n*-hexane, chloroform, ethyl acetate

Determination of total phenolic and flavonoid contents

The total phenolic content (TPC) of the extracts was determined using the Folin–Ciocalteu method as described by Mruthunjaya and Hukkeri [14]. The absorbance was measured at 765 nm and TPC was expressed as mg equivalent of gallic acid per gram of extract (mg GAE/g), using a standard calibration curve established using serial dilutions of gallic acid (2–150 μg/mL).

The total flavonoid content (TFC) of the extracts was determined using the $AlCl_3$ colorimetric assay following method of Nagy et al [15] using rutin as a standard. The absorbance was measured at 510 nm and TFC was expressed as mg rutin equivalent per gram of extract (mg RE/g), using a standard calibration curve established by measuring absorbance of serial dilutions of rutin (20–200 μg/mL). Both experiments were done in triplicate.

Isolation of the major compounds from the root extract

The *n*-hexane fraction (3 g) was chromatographed over silica gel G column (4 cm x 60 cm) using gradient elution which started with *n*-hexane followed by addition of chloroform at 10% increments until 100% chloroform. Subsequently, solvent polarity was increased by addition of 10% increment of EtOAc (10%- 100%). Fractions (100 mL each) were monitored by TLC and similar fractions were pooled together to obtain 4 major fractions, PI-PIV. Fraction PI (0–30% chloroform in *n*-hexane) was subjected to column chromatography using silica gel G eluted with *n*-hexane followed by addition of 10% increments of chloroform till 100% (100 mL fraction each). Similar fractions were pooled and concentrated to yield compound **1** as white powder (50 mg). Compound **2** (white powder, 45 mg) was obtained after recrystallization from fraction PII (300 mg). Fraction PIV (700 mg) eluted with 50–100% EtOAc in chloroform, was subjected to column chromatography using silica gel eluted with a gradient of EtOAc (0– 100%) in chloroform at 10% increments to give compound **3** (reddish yellow oil, 30 mg) and compound **4** (yellow oil, 20 mg).

The ethyl acetate fraction (6 g) was chromatographed on vacuum liquid column (7 cm x 15 cm) packed with silica gel H (200 g). Elution was carried out using chloroform followed by addition of EtOAc by 10% increment to 100%. Afterwards, methanol was added at 5% increments up to 25%. Fractions were monitored by TLC and pooled when appropriate to give 5 fractions EI-EV. Fractions EII and EIV were separately subjected to size exclusion chromatography using sephadex LH-20 eluted with methanol to afford isolation of compound **5** (yellow needles, 80 mg) and compound **6** (white needles, 170 mg), respectively.

Compound **3**: Yellow oil *m/z* 157.1037 for $[M+H]^+$ calculated as $C_{10}H_{21}O$. ^{1}H-NMR,400 MGHz δ_H ppm 0.93 (3H, m, H9), 0.94 (3H, m, H10), 0.97 (3H, m, H8), 0.97 (3H, m, H11),0.99 (3H, d, *J* = 6.9 Hz, H7), 1.23 (1H, br, H3), 1.92 (1H, dh, *J* = 2.5, 6.9 Hz, H6), 3.38 (1H, d, *J* = 2.5 Hz, H2), 3.42 (1H, d, *J* = 10.4 Hz, H5a), 3.54 (1H, d, *J* = 10.4 Hz, H5b).^{13}C-NMR 100 MGHz δ_C ppm 16.5 (C9), 19.8 (C11), 20.3 (C8), 23.5 (C10), 23.6 (C7), 29.2 (C6), 29.6 (C3), 39.4 (C4), 73.3 (C5), 83.5 (C2).

Compound **4**: Yellow orange oil *m/z* 239.0992 corresponding to molecular formula $C_{10}H_{16}NaO_5^+$ for $[M+Na]^+$. ^{1}H-NMR,400 MGHz δ_H ppm 0.97 (3H, m, H7), 0.98 (3H, m, H8), 1.15 (3H, d, *J* = 5.6 Hz, H11), 2.03 (1H, m, H6), 2.55 (1H, m, H3), 3.79 (1H, dd, *J* = 10.9, 2.4 Hz, H5a), 4.09 (1H, dd, *J* = 10.9, 1.4 Hz, H5b), 4.74 (1H, t, *J* = 2.4 Hz, H2).^{13}C-NMR 100

MGHz δ_C ppm 19.9 (C8), 20.3 (C11), 23.2 (C7), 28.8 (C6), 29.6 (C3), 34.5 (C3), 70.8 (C5), 79.3 (C2), .177.4 (C10), 178 (C9).

HPLC analysis of the extracts

Chromatographic analysis was performed on a Dionex chromeleon apparatus equipped with Zobrax eclipse C8 column (4.6 mm X 250 mm, 5 μm) according to the method described previously [16]. The system was operated at column temperature of 30°C and flow rate of 1 mL/min using a binary gradient of 1% aqueous trifluroacetic acid, pH 2.5 (solvent A) and acetonitrile (solvent B). The chromatographic run consisted of two steps gradient: solvent B 5–85% over 40 minutes followed by a slower gradient to 100% B over 15 minutes and an isocratic elution at 100% B for 5 minutes. Eluted peaks were detected at 280 nm for phenolic acids and 360 nm for flavonoids. Each analysis was repeated three times. External standards were analyzed under the same conditions and standard calibration curves for gallic acid and myricetin were plotted using serial dilutions of each (20–200 μg/mL).

Animals

Adult male Wistar Albino rats (180–200 g) were housed at 23 ± 2°C and 55 ± 5% humidity with 12 h light/dark cycle and fed on normal pellet rodent chow and water *ad libitum*. All experimental protocols were approved by the ethical committee for animals' experimentation at Faculty of Pharmacy, Cairo University (July 13th, 2017, protocol No. MP 1432) and followed the Guide for the Care and Use of Laboratory Animals published by the U.S. National Institutes of Health (NIH Publication No. 85–23, revised 1996).

Determination of median lethal dose (LD$_{50}$)

For each extract, 20 rats were allocated into four groups of five rats per group [17]. Each group was orally dosed with a single dose of 100, 500, 1000 and 3000 mg kg^{-1} bwt aerial or root extract. The animals were observed over a period of 48 h for mortality, behavior and signs of toxicity including loss of appetite, vomiting, diarrhea or more than 10% weight loss.

Experimental protocol for assessment of antidiabetic activity

Diabetes was induced in overnight fasted rats (groups **2**–**7**) by subcutaneous injection (s.c.) of streptozotocin (STZ, 50 mg kg^{-1} bwt in 0.1 M citrate buffer, pH 4.5) [18]. After one-week, rats with postprandial blood glucose > 250 mg/dL were selected for the study. Each extract was solubilized in 0.5% aqueous solution of carboxymethyl cellulose (CMC). Rats were randomly divided into seven groups (10 animals each). Group **1** (NC): Normal rats treated with both vehicles (0.1 M citrate buffer, pH 4.5, s.c.) once at the beginning of the experiment and daily oral dose of 0.5% CMC for 21 days. Group **2** (DC): Diabetic rats treated with daily oral dose of 0.5% CMC for 21 days. Groups **3** and **4**: Diabetic rats treated with a daily dose of 250 and 500 mg kg^{-1} bwt of REE, respectively. Groups **5** and **6**: Diabetic rats treated with a daily dose of AEE at 250 and 500 mg kg^{-1} bwt, respectively. Group **7**: Diabetic rats treated with a daily dose of metformin (100 mg kg^{-1} bwt) [19].

Blood glucose level monitoring

Blood was collected after overnight fasting on day 0, 7, 14 and 21 of the experiment from the tail vein. Fasting blood glucose (FBG) was measured using One Touch ULTRA ®Glucometer (LifeScan, Johnson and Johnson, USA). At the end of the experiment, percentage reduction of

the glucose levels at the 21th day was calculated using the following formula:

$$Reduction\ in\ glucose\ level = \frac{FBG21 - FBG0}{FBG0} \text{ X } 100.$$

Where *FBG21* = glycemic value after 21-day treatment, *FBG0* = value at induction. It is denoted as change [A]%.

$$reduction\ in\ glucose\ level\ at\ day\ 21 = \frac{FBGt - FBG[DC]}{FBG[DC]} \text{ X } 100.$$

Where *FBGt* = glycemic value of treated groups, FBG*[DC]* = glycemic value of diabetic group. It is denoted as Change [B]%.

Blood collection and tissue sampling

At the end of treatment, animals fasted overnight and blood was collected from retro-orbital plexus into serum preparation tube [20]. The separated sera were divided into aliquots and stored at -20˚C for insulin assay. The animals were directly decapitated under mild anesthesia after collection of blood samples. At autopsy, pancreases were removed and cleaned from connective tissues, washed in ice-cold 1.15% KCl, and blot dried separately. Pancreases (n = 5) from each group were stored in 10% formalin solution for further histopathological examination. Remaining pancreases (n = 5) were kept at -80˚C for Glut2 and Glut4 assays.

Measurement of serum insulin level

Serum samples were analyzed for insulin using ELISA kit; (kit ref. Rat insulin, Catalog No. MBS724709, San Diego, CA 92195–3308, USA; Sensitivity, 0.1 ng/mL). Experimental procedures followed manufacture's protocol and the kits used have a precision: intra-assay CV (%) and interassay CV (%) less than 10%.

Measurement of Glut2 and Glut4 expressions

Total RNA was extracted from pancreatic tissue samples using Qiagen tissue extraction kit (Qiagen, USA) according to manufacturer's instructions. RNA purity was determined using dual wavelength spectrophotometer (Beckman, USA) and its integrity was examined by running through 1.5% denatured agarose gel. The extracted RNA (0.5–2.0 μg) was converted to cDNA using reverse transcription kit (Fermentas, USA) according to manufacturer's instructions. Three microliters of random primers were added to the 10 μg of RNA. The total volume was adjusted up to 31 μL with DEPC-treated water then incubated in Bio-Rad T100 TM thermal cycler at 65˚C for 10 min. The master mix cDNA was prepared by mixing 5 μL of first strand buffer, 2 μL of 10 mM dNTPs and 1 μL Moloney Murine Leukemia Virus (M-MuLV) reverse transcriptase (50 U/μL). Total volume was adjusted to 19 μL by adding DEPC water to complete volume of master mixture to 50 μL. The mixture was incubated in the programmed thermal cycler for one hour at 37˚C followed by inactivation step at 95˚C for 10 minutes, and finally cooled at 4˚C. Then, RNA changed into cDNA and the converted cDNA were stored at –20˚C for use in real time qPCR.

Real-time qPCR amplification was performed using an Applied Biosystem with software version 3.1 (StepOne™, USA) with the primer sets optimized at the annealing temperature (primer sequences are shown in **Table 1**). For each sample, 1.0 μL forward primer, 1.0 μL reverse primer, 12.5 μL Syber green mix, 5.0 μL cDNA template, and 5.5 μL RNAse free water were added. Running condition for RT-PCR were set as 1 cycle of 2 min at 50˚C and 40 cycles of 15 s at 95˚C, 60 s at 60˚C and 60 s at 72˚C. *β*-Actin mRNA was used as a reference. PCR

Table 1. The primer sequence of the studied genes.

Target gene	Primer sequence
Glut4	Forward primer: 5'-CAACTGGACCTGTAACTTCATTGT-3' Reverse primer: 5'-ACGGCAAATAGAAGGAAGACGTA-3
Glut2	Forward primer:5'-AAGGATCAAAGCCATGTTGG -3' Reverse primer:5'-GGAGACCTTCTGCTCAGTGG-3'
Beta actin	Forward primer:5'-CAG GAT GGC GTG AGG GAG AGC-3' Reverse primer: 5'-AAG GTG TGA TGG TGG GAA TGG-3'

products were photographed and subjected to band intensity analysis using Applied Bio system software. The method of $2^{-\Delta\Delta Ct}$ was adopted for analysis.

Histopathological examination of pancreas

Pancreas tissues were fixed in 10% formalin saline for 24 hours then washed in tap water followed by washing in serial dilutions of alcohol for dehydration. Specimens were cleared in xylene and embedded in paraffin at 56°C in hot air oven for 24 h. Paraffin bees wax tissue blocks were prepared for sectioning at 4 microns thickness by sledge microtome. The obtained tissue sections were collected on glass slides, deparaffinized, and stained by hematoxylin & eosin stain for routine examination through light electric microscope [21].

DPPH radical scavenging assay

DPPH free radical scavenging assay was performed as described previously [22]. DPPH in methanol (0.02 mg/mL) was incubated with different concentrations of AEE and REE for 30 min in dark and the reduction in color was measured at 517 nm using spectrophotometer. The percentage of DPPH radical scavenging (I) was calculated as follows

$$I = \left(1 - \frac{Ac}{At}\right) \times 100$$

Where **At** = absorbance of the tested extracts, **Ac** = absorbance of control (DPPH solution without the tested extract). Ascorbic acid was used as a standard antioxidant and showed IC_{50} of 8.5 μg/mL.

α-glucosidase inhibitory assay

α-Glucosidase enzyme inhibitory activity was determined using the method reported by You et al. [23]. Serial dilution of REE and AEE (7.81–1000 μg/mL) were incubated with 500 μL of 1 U/mL α-glucosidase solution. *p*-Nitrophenyl glucopyranoside (*p*-NPG), 5 mM was used as a substrate. Released *p*-nitrophenol was estimated by measuring absorbance at 405 nm. Acarbose was used as a positive control at the same concentrations.

The percentage of inhibition was calculated using the following formula:

$$\% \text{ inhibition} = \left(1 - \frac{Abs\ control}{Abs\ sample}\right) \times 100$$

Where: **Abs control**: absorbance of the control reaction (containing all reagent except the test sample); **Abs sample**: absorbance of the test sample.

Each experiment was performed in triplicate and concentrations that caused 50% inhibition (IC_{50}) were calculated from response curve.

α-amylase inhibitory assay

Inhibition of α-*amylase* enzyme was determined using the method reported by Narkhede et al. [24].

Briefly, 1 mL of the REE and AEE of various concentrations (7.81–1000 μg/mL) and 1 mL of enzyme solution (0.5 mg/mL) were mixed together and incubated at 25˚C for 10 min. Then, 1 mL of starch solution (0.5%) was added and the mixture was further incubated at 25˚C for 10 min. The reaction mixture was then stopped by adding 2 mL of dinitrosalicylic acid (DNS) followed by heating the reaction mixture in a boiling water bath (5 min). After cooling, the absorbance was measured at 565 nm. The percentage of inhibition was calculated as mentioned for α-glucosidase assay.

Molecular docking

Molecular docking studies were performed using Molecular Operating Environment MOE platform, 2015.1. (Chemical Computing Group, Canada). 3D structures of the tested compounds were introduced using the builder interface of MOE. Partial charges were added and energy minimization was performed using MMFF94x force field. The structure of human glycerol-3-phosphate dehydrogenase, GPDH, co-crystallized with dihydroxy acetone phosphate (DHAP) was downloaded from protein databank, code 1WPQ, (https://www.rcsb.org). After hydrogen addition and energy minimization, the co-crystallized ligand was removed and redocked to RMSD 0.8591 Å. Molecules were docked in the active sites of GPDH using triangle matcher placement method and their docking score was calculated using London dG function.

Statistical analysis

All data were represented as mean ± standard error (SE); the results were analyzed by One-Way (ANOVA), with post hoc Tukey test. Differences were considered statistically significant at $P < 0.05$. The data analyses were conducted using GraphPad Prism7 (GraphPad Software, San Diego CA, USA).

Results and discussion

The LD_{50} study carried on rats revealed no mortality among animals and no signs of toxicity up to 3000 mg kg^{-1} bwt of both extracts. Animals that received streptozotocin (STZ) showed clear hyperglycaemia manifested by FBG > 400 mg/dL. At day-21, treatment with REE at high and low doses (500 and 250 mg kg^{-1} bwt) exhibited a significant decrease in glucose level by -44%, and -39%, respectively, compared to control diabetic group (DC). Furthermore, treatment with AEE at high dose and low dose (500 and 250 mg kg^{-1} bwt) significantly diminished glucose level by -41% and -37%, respectively. Compared to the groups at their respective day zero, treatment with REE at high and low doses (500 and 250 mg kg^{-1} bwt) exhibited a significant decrease in glucose level by -31.48%, and -7%, respectively. Moreover, treatment with AEE at high dose and low dose (500 and 250 mg kg^{-1} bwt) significantly reduced glucose level by -5.51% and -6.88%, respectively (**Table 2**). Collectively, REE at a dose of 500 mg kg^{-1} bwt was most effective in attenuating glycaemic status than other investigated treatments except the standard drug metformin (MF).

In attempt to further explore the basis for the antidiabetic action of both extracts, level of serum insulin as well as expression levels of two glucose transporters Glut2 and Glut4 in the pancreatic tissue were estimated. Glucose transporters are specific facilitative glucose carrier proteins including glucose transporter 2 and 4 (Glut2 and Glut4) which are expressed in liver,

Table 2. Effect of REE, AEE and metformin on serum glucose concentration (mg/dL) in diabetic adult male rats.

Group	Zero-	Day-7	Day-14	Day-21	Change^A%	Change^B%
NC	78.13 ± 8.32	79.88 ± 7.45	85.88 ± 8.0	87.50 ± 7.2		
DC	429.40 ± 86.4	438.2 ± 85.3	465.6 ± 60.6	527.0 ± 58.7	22.73	
DC + MF	319.0 ± 117.1	262.33 ± 127.0	221.83 ± 114.9	181.67 ± 29.3^{a*b***}	-43.05	-66%
DC + REE (500)	428.33 ± 83.1	375.33 ± 74.2	331.67 ± 58.7	293.5 ± 55.^{a*b**}	-31.48	-44%
DC + REE (250)	350.25 ± 133.6	310.24 ± 137.9	335.36 ± 178.9	323.68 ± 178.3^{b**}	-7.59	-39%
DC + AEE (500)	356.0 ± 125.3	285.2 ± 115.2	264.6 ± 105.6	312.0 ± 127.6^{b*}	-5.51	-41%
DC + AEE (250)	357.43 ± 131.57	347.43 ± 131.2	308.0 ± 94.9	332.83 ± 86.5^{b*}	-6.88	-37%

^{a}; represent significance from their respective controls at zero-time

^{b}; represent significance from diabetic group (DC) at 21-day.

$^*p < 0.05$

$^{**}p < 0.01$ and

$^{***}p < 0.001$

Animals group are designated as: **NC**: normal control, **DC**: diabetic control, **DC + MF**: diabetic animals that received daily dose of metformin 100 mg kg^{-1} bwt, **DC + REE**: diabetic animals that received daily dose of root ethanol extract, **DC + AEE**: diabetic animals that received aerial part ethanol extract.

Change$^{(A)}$: change in glycemic value in treated groups at day 21 from its respective day zero.

Change$^{(B)}$: Change in glycemic value in day 21 from the value in diabetic group (DC) in day 21.

intestine, kidney, and β-pancreatic islet cells [25]. In the current study, severe depletion in serum insulin and down regulation in Glut2 and Glut4 were observed in diabetic animals as low levels of these transporters will limit uptake of circulating glucose into pancreases and other tissues causing decreased insulin secretion and hyperglycaemia [26]. When compared to metformin (MF) which exerts its antidiabetic effect by increasing glucose consumption and insulin sensitivity, administration of REE at both doses augmented insulin level and up-regulated expression of Glut2 and Glut4 to comparable levels (**Table 3**). Meanwhile, administration of AEE at the same dose showed only negligible increase in insulin level, Glut2 and Glut4

Table 3. Effect of REE and AEE on insulin level and glucose transport in diabetic rats.

Group	Insulin (µU/mL)	Glut 2	Glut4
NC	80.69 ± 8.65	1.01 ± 0.02	1.02 ± 0.03
DC	28.91 ± 2.12 ^{a***}	0.18 ± 0.09 ^{a***}	0.20 ± 0.02^{a***}
DC + MF	52.16 ± 7.96 ^{a***b***}	0.72 ± 0.13 ^{b***}	0.63 ± 0.06^{a***b***}
DC + REE (500)	62.06 ± 3.71 ^{a*b***}	0.83 ± 0.08^{b***}	0.64 ± 0.06^{a*b***}
DC + REE (250)	54.76 ± 5.76 ^{a***b***}	0.83 ± 0.05 ^{b***}	0.69 ± 0.05 ^{a***b***}
DC + AEE (500)	31.99 ± 2.36 ^{a***c**}	0.19 ± 0.11 ^{a***c***}	0.23 ± 0.05 ^{a***c***}
DC + AEE (250)	36.41 ± 4.56^{a***c*}	0.22 ± 0.17^{a***c***}	0.23 ± 0.06 ^{a***c***}

^{a}; Significance from their respective controls at zero time.

^{b}; significance from diabetic group.

^{c}; significance from reference drug (metformin)

$^*p < 0.05$

$^{**}p < 0.01$ and

$^{***}p < 0.001$

Glut2: glucose transporter-2, **Glut4**: glucose transporter 4. Animals group are designated as: **NC**: normal control, **DC**: diabetic control, **DC + MF**: diabetic animals that received daily dose of metformin 100 mg kg^{-1} bwt, **DC + REE**: diabetic animals that received daily dose of root ethanol extract, **DC + AEE**: diabetic animals that received aerial part ethanol extract.
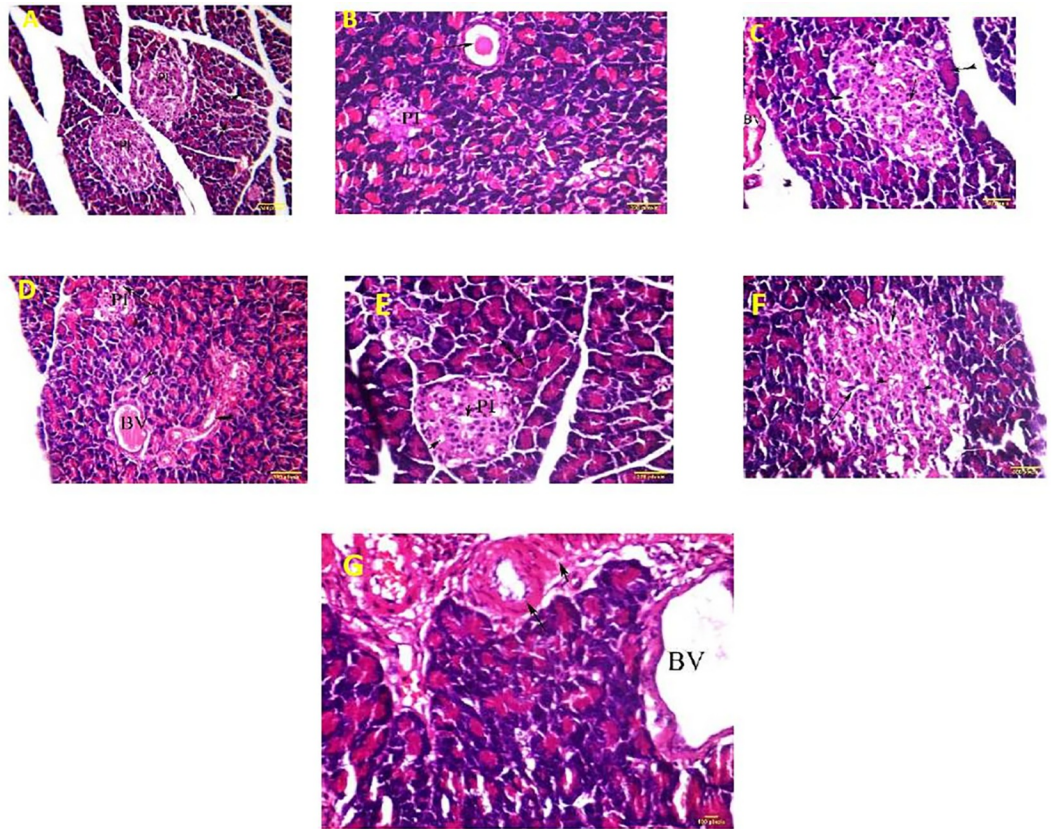
Fig 1. Photomicrographs of rat pancreases isolated from different animal groups. Photomicrographs of cross section of the pancreatic tissue of **A**: normal healthy animals showing normal pancreatic islets (PI) and pancreatic acini (arrow), **B**: diabetic group showing pancreatic duct inspissiated (arrow), pancreatic islet (pi) with sever reduction in size and hypocellularity. **C**: animals treated with REE 250 mg/kg showing: pancreatic islet (short arrow), inspissated pancreatic duct (long arrow) and blood vessel (double arrow) and pancreatic acini (arrow head). **D**: animals treated with REE 500 mg kg^{-1} bwt showing pancreatic islet moderate in size and dilated congested blood vessel (arrow). **E**: animals treated with 250 mg kg^{-1} bwt AEE showing pancreatic blood vessels with thickened walls (arrow) and perivascular fibrotic reaction (short arrow). **F**: animals treated with AEE (500 mg kg^{-1} bwt) showing islets with normal size and vaccuolation between cells (arrowhead), pancreatic duct (arrow). (H & E). **G**: Animals treated with metformin showing: pancreatic islets with vacuolation between cells (arrow), dilated congested blood vessel (BV), and intact pancreatic acini (double arrow).

expression further confirming variability in the antidiabetic effect of both extracts which appeared to be mediated, at least partially, by increased glucose uptake in case of REE.

Histopathological examination was conducted on the pancreatic tissue in various animal groups. Diabetic untreated animals showed many pathological alterations in the pancreatic tissue compared with non-diabetic animals manifested by severe reduction in the number and size of pancreatic islets with hypocellularity, dilated congested capillaries and mild vacuolation in and between cells (**Fig 1A and 1B**). Significant improvement was observed in the group treated with MF, where many pancreatic islets were normal in size and cellularity (**Fig 1C**). In the groups treated with REE at both doses, only few cells displayed atrophies with degenerative changes and mild hypocellularity was observed (**Fig 1C and 1D**). Meanwhile, animals treated with high dose of AEE showed mild to moderate pathological changes, where pancreatic islets with dilated capillaries and vacuolation were observed and occasional islets displayed reduction in size (**Fig 1E**), while lower dose of AEE failed to produce significant amelioration of tissue damage (**Fig 1F**).

Table 4. Chemical characterization of REE and AEE and their ethyl acetate fractions.

Compounds	Root		Aerial parts	
	Ethanol Ext	EtOAc Fr.	Ethanol Ext	EtOAc Fr.
Total phenolics[a]	252.6 ± 0.04	nd	124 ± 0.22	nd
Total flavonoids[b]	20.326 ±0.023	nd	26.6 ± 0.0819	nd
Gallic acid[c]	3.46 ± 0.05	9.026 ± 0.01	20.6 ± 0.03	8.5 ± 0.005
Myricetin[c]	5.6 ± 0.014	7.85 ± 0.002	10.0 ± 0.004	6.0 ± 0.001
Umbelliferone[c]	10.0 ± 0.008	6.35 ± 0.001	1.30 ± 0.001	-

EtOAc Fr = Ethyl acetate fraction, Ext = extract, nd = not determined

[a]: mg GAE/g

[b]: mg RE/g

[c]:μg/mL

Values are expressed as means ± S.E., n = 3

Moreover, *Limonium axillare* root extract (REE) was highly enriched in phenolic compounds with total phenolic content of 252 mg GAE/g of extract compared to 124 ± 2.129 mg GAE/g for AEE. Meanwhile, AEE showed higher TFC (26.6 mg QE/g) than REE (**Table 4**). This resulted in a good *in vitro* radical scavenging activity of REE (IC_{50} = 25.2 μg/mL) compared to much weaker activity of AEE with IC_{50} of 407.9 μg/mL explaining to a certain extent the preservation of pancreatic tissue integrity in animals receiving REE rather than AEE. STZ is thought to induce diabetes by liberation of superoxide radicals which then cause DNA damage and subsequent β-cells necrosis [18]. Therefore, strong radical scavenging activity of the extract can ameliorate its detrimental effect.

Additionally, REE, AEE and their fractions were evaluated for possible inhibition of α-glucosidase and pancreatic α-amylase, two enzymes involved in releasing glucose from dietary carbohydrates. Among investigated samples, REE, its EtOAc fraction and AEE showed the most potent inhibition of α-glucosidase enzyme with IC_{50} values at 44.8, 59 and 60.4 μg/mL, respectively, compared to acarbose (IC_{50} = 30.57 μg/mL), **Table 5**. Similar results were obtained in pancreatic α-amylase inhibition assay, where *n*-hexane fraction of REE and EtOAc fractions of both REE and AEE showed strong inhibition of α-amylase with IC_{50} values at 41.6, 45.8 and 48.1 μg/mL, respectively (IC_{50} of acarbose was observed at 34.71 μg/mL), **Table 5**.

Table 5. α-glucosidase and α-amylase inhibitory activity of REE and AEE and their fractions measured as IC_{50} (μg/mL).

Sample		IC_{50} α-glucosidase	IC_{50} α-amylase
REE	Total extract	44.8	89.3
	n-hexane Fr.	89.3	41.6
	DCM Fr.	426.04	192.13
	EtOAc Fr.	59.0	45.8
	n-Butanol	229.3-	115.9
AEE	Total extract	60.4	115.99
	n-hexane Fr.	123.7	NA
	DCM Fr.	341.9	111.6
	EtOAc Fr.	192.2	48.13
	n-Butanol	47.7	805.9

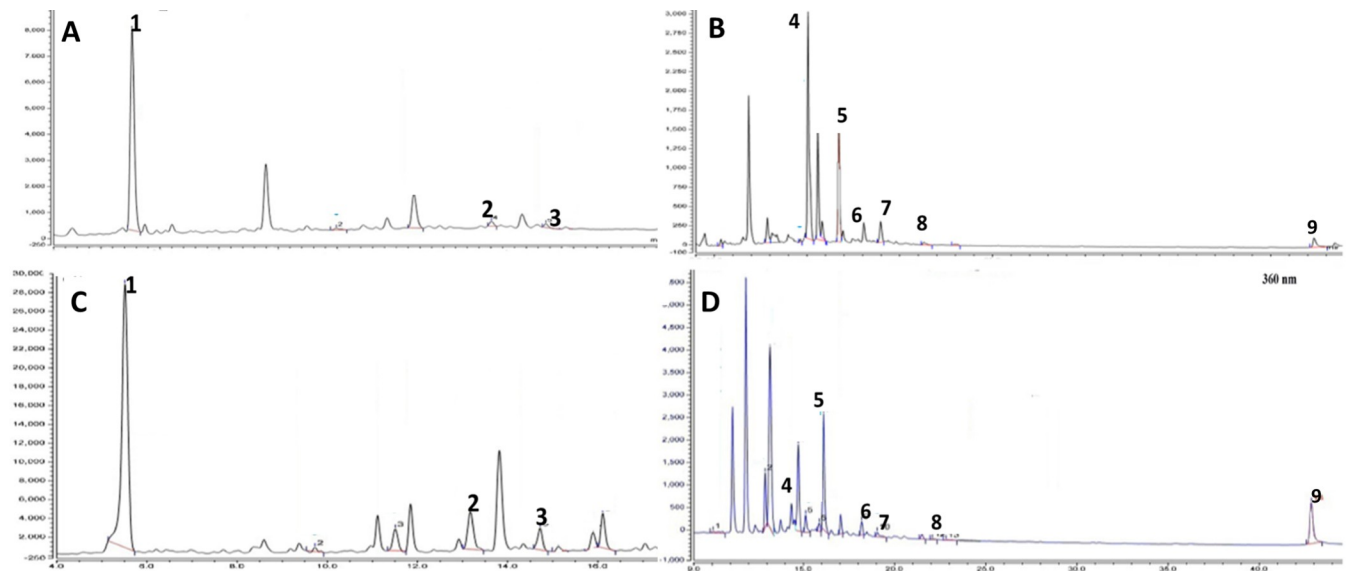DCM: dichloromethane, EtOAc: ethyl acetate, Fr: fraction, NA: not active

Fig 2. HPLC chromatograms for AEE and REE at λ = 280 and 360 nm. A and **B**:HPLC analysis for REE showing eluted compounds with UV absorbance at λ = 280 and 360 nm, respectively. **C** and **D**: HPLC chromatogram of eluted compounds detected at λ = 280 and 360, respectively. Identified compounds are labeled as **1**: gallic acid, **2**:ellagic acid, **3**: ferulic acid, **4**: umbelliferone, **5**: myricetin, **6**:quercetin, **7**:coumarin, **8**:apigenin and **9**:kaempferol.

These findings indicate that inhibition of these enzymes may be a contributing mechanism in the antidiabetic activity of both extracts. It is worth mentioning that several *Limonium* species have shown strong *in vitro* inhibitory activity against both α-glucosidase and pancreatic α-amylase [27, 28].

HPLC analysis of both extracts using external standards previously isolated from the plant identified umbelliferone and gallic acids as the major constituents in REE (**Fig 2**), while AEE was enriched with the flavonoid myricetin in addition to gallic acid. Myricetin and its glycosides have been reported in other *Limonium* species including *L. gmelinii* and *L. bicolor* [29, 30]. Moreover, myricetin was found to accumulate in roots of *L. bicolor* in response to salt stress [31] Literature has shown that leaves of different amaranth species, such as *A. gangeticus*, drought-tolerant leafy vegetable amaranth, and *A. tricolor* had abundant gallic acids [32–34]. Similarly, leaves of salt-tolerant vegetable amaranth, *A. tricolor*, drought-tolerant vegetable amaranth, and red amaranth had abundant myricetin which is corroborative to the present findings [35, 36]. Other identified metabolites included ellagic acid, ferulic acid, kaempferol, quercetin, coumarin and apigenin which all have been reported in the plant previously [12, 37] (**Fig 2**). Myricetin and quercetin are known inhibitors of both α-glucosidase and α-amylase partially explaining *in vitro* assay results and likely contributing to antidiabetic activity of the extract by diminishing the release of glucose from dietary carbohydrates [38]. Meanwhile, gallic and ellagic acids and flavonoids are potent antioxidants which can offset the detrimental effect produced by superoxide radicals released as a result of STZ intoxication [39–41].

To follow up on the bioactive fractions, *n*-hexane and EtOAc fractions were subjected to repeated column chromatography which led to the isolation of six compounds including four known compounds, namely *β*-sitosterol-*3-O*-palimtate (**1**) and *β*-sitosterol (**2**) from *n*-hexane fraction and myricetin (**5**) and gallic acid (**6**) from EtOAc fraction (**Fig 3**). Additionally, two new compounds were isolated from the *n*-hexane fraction and are designated here as compounds **3** and **4.** All compounds were identified based on their chromatographic behaviours and 1D and 2D-NMR data. For compound **3**, ^{1}H and ^{13}C NMR spectra did not show any
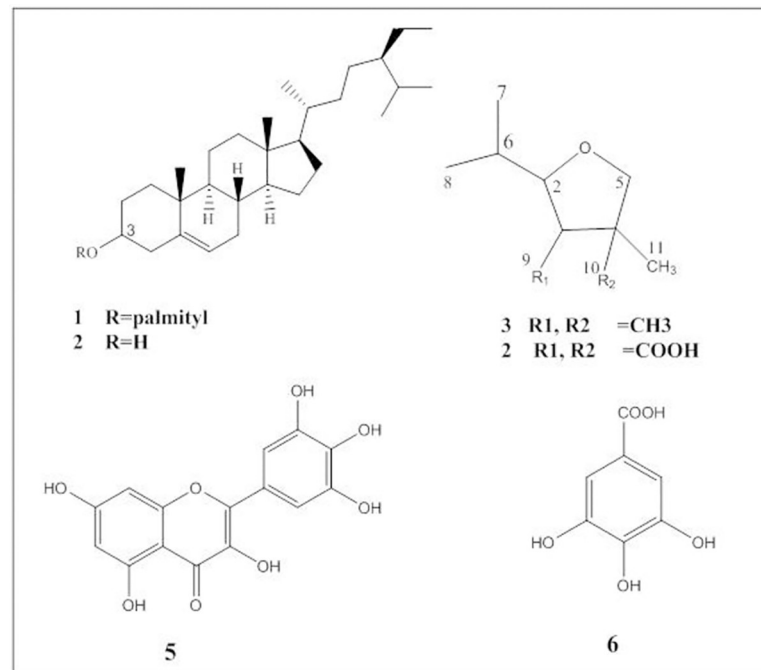
Fig 3. Compounds isolated from the root extract of *Limonium axillare*.

signals above δ_H 3.6 and δ_C above 84, respectively suggesting a tetrahydrofuran ring structure with no functional group substituents. ^{1}H-^{1}H-COSY and ^{1}H-^{13}C correlation spectra established the connectivity between various substituents as illustrated in **S1-S3 Figs in S1 File** and compound **3** was chemically identified as 1-isopropyl- 3,4,4, trimethyl-tetrahydrofuran (**Fig 3**). In higher plants, tetrahydrofuran-terpenes and sesquiterpenes are components responsible for aroma including several tetrahydrofuran predominately isolated from wine and grapes [42].

The ^{13}C-NMR spectrum and MS analysis of compound **4** indicated the presence of two carboxylic groups δ_C 177.4 and 178, which resulted in downfield shifts of H2, H3 and H5. Analysis of 2D-correlation spectra (**S4-S6 Figs in S1 File**) identified compound **4** as 2-isopropyl-4-methyltetrahydrofuran-3,4-dicarboxylic acid, which is reported for the first time (**Fig 3**).

Finally, we used molecular docking to investigate possible affinity of major REE constituents to glycerol-3-phosphate dehydrogenase GPDH, a newly identified target for metformin which inhibition leads to suppression of gluconeogenesis [43]. Potential inhibitors that were identified for GPDH include chalcone derivatives and some flavonoids which showed good inhibitory activity for bacterial and protozoal GPDH [44, 45]. Docking of 2',4' dihydroxychalcone in the active site of human GPDH revealed a key hydrogen bond interaction with Arg269, which is a key residue in interacting with the phosphate group of its substrate dihydroxy acetone phosphate (DHAP). Other interactions of dihydroxychalcone included two other key amino acid residues Lys120, which stabilizes the hydroxyl and carbonyl oxygen of DHAP and Leu118, which is involved in interaction with NAD [46]. Among the compounds isolated from REE, myricetin, showed better docking score than dihydroxychalcone (**Table 6**) with possible interaction with Arg269, Leu118, Lys120 and Ile152. Metformin, compound **3** and compound **4** showed at least one interaction with these key amino acid residues (**Fig 4**).

Based on the chemical profiles and biological assessment of both REE and AEE extracts, the ethanobotanical use of the roots of *Limonium axillare* seem to be justified. While extract of the

Table 6. Molecular docking results and ligand inteactions of major phytoconstituents of *Limonium axillare* root extract in active site of glycerol-3-phosphate in comparison with known inhibitors.

Ligand	Docking score kcal/mol	Residue	Type of interaction
2',4'Dihydroxychalcone	-6.2652	Leu118	H-bond
		Lys120	H$^+$ arene
		Arg269	H-bond
Metformin	-4.6791	Arg269	H-bond
Gallic acid	-4.903	Gly10	H-bond
		Ser11	H-bond
		Gly294	H-bond
Myrecitin	-6.6121	Lys120	H-bond
		Ile152	H$^+$ arene
Compound 3	-5.6075	Arg269	H-bond
Compound 4	-5.7992	Lys120	H-bond
		Asn205	H-bond

https://doi.org/10.1371/journal.pone.0255904.t006

aerial part showed mild antidiabetic activity, likely mediated through inhibition of α-glucosidase and α-amylase, antidiabetic action of root extract may be mediated through multiple mechanisms including antioxidant activity, enhanced insulin secretion, in addition to marked increase in expression of Glut2 and Glut4 and therefore increasing glucose uptake. We also provided evidence from *in silico* studies to suggest that constituents of root extract may have binding affinity to glycerol-3-phosphate dehydrogenase. The study encourages further investigation of the antidiabetic effects of *L. axillare* as it is likely to be affected by the plant habitat and its geographical origin. Also, it should be noted that other underlying mechanism for
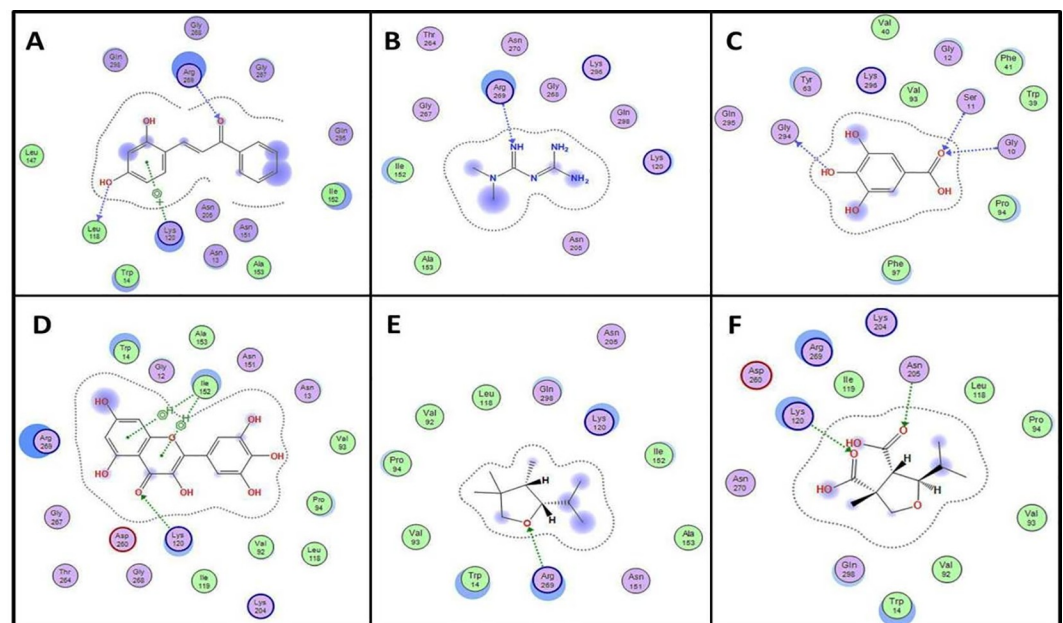

Fig 4. Enzyme ligand interactions of *Limonium axillare* phytoconstituents in the active site glycerol phosphate dehydrogenase. Diagrams representing 2D enzyme ligand interaction in the active site of GPDH with tested compounds A: 2',4' dihydroxychalcone, B: metformin, C: gallic acid, D: myricetin, E: compound **3**, F: compound **4**.

https://doi.org/10.1371/journal.pone.0255904.g004

antidiabtic activity may also be involved. It is not clear from the current study, if the anti-hyperglycemic action of *L. axillare* can be sustained over a period of time and whether it can prevent other complications of DM, which ought to be addressed in future studies. We would like to point out that under-investigated flora are potential repertoires of novel natural products with possible biological activities and our study underscores the importance of experimental investigations of unexplored ethnobotanical remedies either by classic phytochemical investigation or through comprehensive metabolomics studies.

Supporting information

S1 File. NMR spectra for both compound 3 and 4.
(DOCX)

Acknowledgments

The authors thank Prof. Hiroyuki Morita at Institute of Natural Medicine, University of Toyama, Japan for acquiring high resolution MS data.

Author Contributions

Conceptualization: Essam Abdel-Sattar, Engy A. Mahrous.

Data curation: Manal M. Shams, Marwa M. Abd-Rabo, Nehad Mahmoud.

Investigation: Manal M. Shams, Marwa M. Abd-Rabo, Nehad Mahmoud.

Methodology: Manal M. Shams, Marwa M. Abd-Rabo, Nehad Mahmoud, Engy A. Mahrous.

Supervision: Essam Abdel-Sattar, Engy A. Mahrous.

Validation: Marwa M. Abd-Rabo.

Visualization: Essam Abdel-Sattar.

Writing – original draft: Manal M. Shams, Marwa M. Abd-Rabo, Nehad Mahmoud.

Writing – review & editing: Essam Abdel-Sattar, Engy A. Mahrous.

References

1. Orasanu G, Plutzky J. The pathologic continuum of diabetic vascular disease. J Am Coll Cardiol. 2009; 53: S35–S42. https://doi.org/10.1016/j.jacc.2008.09.055 PMID: 19179216

2. Doliba NM. Pancreatic islet adaptation and failure in obesity and diabetes. Metabolic Syndrome. Springer International Publishing; 2017. pp. 1–21. https://doi.org/10.1007/978-3-319-12125-3_27–2

3. Hago S, Mahrous EA, Moawad M, Abdel-Wahab S, Abdel-Sattar E. Evaluation of antidiabetic activity of *Morus nigra* L. and *Bauhinia variegata* L. leaves as Egyptian remedies used for the treatment of diabetes. Nat Prod Res. 2021; 35: 829–835. https://doi.org/10.1080/14786419.2019.1601094 PMID: 30968706

4. Elbanna A, Nooh M, Mahrous E, Khaleel A, Elalfy T. Extract of *Bauhinia vahlii* shows antihyperglycemic activity, reverses oxidative stress, and protects against liver damage in streptozotocin-induced diabetic rats. Pharmacogn Mag. 2017; 13: 607. https://doi.org/10.4103/pm.pm_53_17 PMID: 29200721

5. Hemming CF. The ecology of the coastal area of Northern Eritrea. J Ecol. 1961; 49: 55–78. https://doi.org/10.2307/2257423

6. Phondani PC, Bhatt A, Elsarrag E, Horr YA. Ethnobotanical magnitude towards sustainable utilization of wild foliage in Arabian Desert. J Tradit Complement Med. 2016; 6: 209–218. https://doi.org/10.1016/j.jtcme.2015.03.003 PMID: 27419083

7. Mahmoud T, Gairola S. Traditional knowledge and use of medicinal plants in the Eastern Desert of Egypt: a case study from Wadi El-Gemal National Park. J Med Plants Stud. 2013; 1: 10–17.

8. Tounekti T, Mahdhi M, Khemira H. Ethnobotanical study of indigenous medicinal plants of Jazan region, Saudi Arabia. Evidence-Based Complement Altern Med. 2019; 2019: 1–45. https://doi.org/10.1155/2019/3190670 PMID: 31275409

9. Akbar S, Al-Yahya MA. Screening of Saudi plants for phytoconstituents, pharmacological and antimicrobial properties. Aust J Med Herbal. 2011; 23: 76–87:

10. Bouftira I, Hajari S Al, Abdelly PC, Sfar PS. Antioxidative and free radical of *Limonium axillare* from Qatarian coasts Webmed Cent. 2010; 1: 1–9.

11. Mahasneh AM. Screening of some indigenous Qatari medicinal plants for antimicrobial activity. Phyther Res. 2002; 16: 751–753. https://doi.org/10.1002/ptr.1037 PMID: 12458480

12. Ahmed KM, Kandil FE, Mabry TJ. An anticancer tannin and other phenolics from *Limonium axaillare* (Fam. Plumbaginaceae). Asian J Chem. 1999; 11: 261–263.

13. Bashir A., Abdalla AA, Wasfi IA, Hassan ES, Amiri MH, Crabb TA. Flavonoids of *Limonium axillare*. Int J Pharmacogn. 1994; 32: 366–372. https://doi.org/10.3109/13880209409083017

14. Mruthunjaya K, Hukkeri VI. In vitro antioxidant and free radical scavenging potential of *Parkinsonia aculeata* Linn. Pharmacogn Mag. 2008; 4: 42–51.

15. Nagy M, Tofană M, Socaci SA, Pop AV, Borş MD, Fărcaş A, et al. Total phenolic, flavonoids and antioxidant capacity of some medicinal and aromatic plants. Bull Univ Agric Sci Vet Med Cluj-Napoca Food Sci Technol. 2014. https://doi.org/10.15835/buasvmcn-fst:10639

16. Menghinello P, Cucchiarini L, Palma F, Agostini D, Dachà M, Stocchi V. Simultaneous analysis of flavonoid aglycones in natural products using an RP-HPLC method. J Liq Chromatogr Relat Technol. 1999; 22: 3007–3018. https://doi.org/10.1081/JLC-100102074

17. Lorke D. A new approach to practical acute toxicity testing. Arch Toxicol. 1983; 54: 275–287. https://doi.org/10.1007/BF01234480 PMID: 6667118

18. Szkudelski T. The mechanism of alloxan and streptozotocin action in B cells of the rat pancreas. Physiol Res. 2001; 50: 537–46. PMID: 11829314

19. Cheng JT, Huang CC, Liu IM, Tzeng TF, Chih JC. Novel mechanism for plasma glucose-lowering action of metformin in streptozotocin-induced diabetic rats. Diabetes. 2006; 55: 819–825. https://doi.org/10.2337/diabetes.55.03.06.db05-0934 PMID: 16505249

20. Schermer S. The blood morphology of laboratory animals 3d ed. Sainte-Foy, Québec: Université Laval, Faculté des sciences sociales; 1967. PMID: 6081056

21. Brancroft JD, Stevens A. Theory and practice of histological technniques. 1982. Elseiver, Amesterdam.

22. Viturro C, Molina A, Schmeda-Hirschmann G. Free radical scavengers from *Mutisia friesiana* (Asteraceae) and *Sanicula graveolens* (Apiaceae). Phyther Res. 1999; 13: 422–424. https://doi.org/10.1002/(SICI)1099-1573(199908/09)13:5<422::AID-PTR462>3.0.CO;2-M

23. You Q, Chen F, Wang X, Luo PG, Jiang Y. Inhibitory effects of muscadine anthocyanins on α-glucosidase and pancreatic lipase activities. J Agric Food Chem. 2011; 59: 9506–9511. https://doi.org/10.1021/jf201452v PMID: 21797278

24. Narkhede MB, Ajimire P V., Wagh AE, Mohan M, Shivashanmugam A. In vitro antidiabetic activity of *Caesalpina digyna* (R.) methanol root extract. Asian J Plant Sci Res. 2011; 1: 101–106.

25. Villanueva-Peñacarrillo ML, Puente J, Redondo A, Clemente F, Valverde I. Effect of GLP-1 treatment on GLUT2 and GLUT4 expression in type 1 and type 2 rat diabetic models. Endocrine. 2001; 15: 241–248. https://doi.org/10.1385/ENDO:15:2:241 PMID: 11720253

26. Thorens B. GLUT2, glucose sensing and glucose homeostasis. Diabetologia. 2015; 58: 221–232. https://doi.org/10.1007/s00125-014-3451-1 PMID: 25421524

27. Mazouz W, Haouli NEH, Gali L, Vezza T, Bensouici C, Mebrek S, et al. Antioxidant, anti-alzheimer, antidiabetic, and anti-inflammatory activities of the endemic halophyte *Limonium spathulatum* (Desf.) kuntze on LPS-stimulated RAW264 macrophages. South African J Bot. 2020; 135: 101–108. https://doi.org/10.1016/j.sajb.2020.08.021

28. Senizza B, Zhang L, Rocchetti G, Zengin G, Ak G, Yıldıztugay E, et al. Metabolomic profiling and biological properties of six *Limonium* species: novel perspectives for nutraceutical purposes. Food Funct. 2021; 12: 3443–3454. https://doi.org/10.1039/d0fo02968h PMID: 33900332

29. Kozhamkulova Z, Radwan M, Zhusupova G, Abilov Z, Rahadilova S, Ross S. A new flavonol glycoside from *Limonium gmelinii*. Planta Med. 2010; 76. https://doi.org/10.1055/s-0030-1251829 PMID: 20734940

30. Chen J, Teng J, Ma L, Tong H, Ren B, Wang L, et al. Flavonoids isolated from the flowers of *Limonium bicolor* and their in vitro antitumor evaluation. Pharmacogn Mag. 2017; 13: 222–225. https://doi.org/10.4103/0973-1296.204566 PMID: 28539711

31. Wang L, Li W, Ma L, Chen J, Lü H, Jian T. Salt stress changes chemical composition in *Limonium bicolor* (Bag.) Kuntze, a medicinal halophytic plant. Ind Crops Prod. 2016; 84: 248–253. https://doi.org/10.1016/j.indcrop.2016.01.050

32. Sarker U, Oba S. Polyphenol and flavonoid profiles and radical scavenging activity in leafy vegetable *Amaranthus gangeticus*. BMC Plant Biol. 2020; 20: 499. https://doi.org/10.1186/s12870-020-02700-0 PMID: 33138787

33. Sarker U, Oba S. Phenolic profiles and antioxidant activities in selected drought-tolerant leafy vegetable amaranth. Sci Rep. 2020; 10: 18287. https://doi.org/10.1038/s41598-020-71727-y PMID: 33106544

34. Sarker U, Oba S. Augmentation of leaf color parameters, pigments, vitamins, phenolic acids, flavonoids and antioxidant activity in selected *Amaranthus tricolor* under salinity stress. Sci Rep. 2018; 8: 12349. https://doi.org/10.1038/s41598-018-30897-6 PMID: 30120319

35. Sarker U, Hossain MN, Iqbal MA, Oba S. Bioactive components and radical scavenging activity in selected advance lines of salt-tolerant vegetable Amaranth. Front Nutr. 2020; 7. https://doi.org/10.3389/fnut.2020.587257 PMID: 33330589

36. Sarker U, Oba S. Antioxidant constituents of three selected red and green color Amaranthus leafy vegetable. Sci Rep. 2019; 9: 18233. https://doi.org/10.1038/s41598-019-52033-8 PMID: 31796754

37. Kandil FE, Ahmed KM, Hussieny HA, Soliman AM. A New Flavonoid from *Limonium axillare*. Arch Pharm (Weinheim). 2000; 333: 275–277. https://doi.org/10.1002/1521-4184(20008)333:8<275::aid-ardp275>3.0.co;2-4 PMID: 11008378

38. Ng K. Evaluation of α-amylase and α-glucosidase inhibitory activity of flavonoids. Int J Food Nutr Sci. 2016; 2: 1–6. https://doi.org/10.15436/2377-0619.15.042

39. Priyadarsini KI, Khopde SM, Kumar SS, Mohan H. Free radical studies of ellagic acid, a natural phenolic antioxidant. J Agric Food Chem. 2002; 50: 2200–2206. https://doi.org/10.1021/jf011275g PMID: 11902978

40. Sroka Z, Cisowski W. Hydrogen peroxide scavenging, antioxidant and anti-radical activity of some phenolic acids. Food Chem Toxicol. 2003; 41: 753–758. https://doi.org/10.1016/s0278-6915(02)00329-0 PMID: 12738180

41. Boots AW, Haenen GRMM, Bast A. Health effects of quercetin: From antioxidant to nutraceutical. Eur J Pharmacol. 2008; 585: 325–337. https://doi.org/10.1016/j.ejphar.2008.03.008 PMID: 18417116

42. Marais J. Terpenes in the aroma of grapes and wines: A Review. South African J Enol Vitic. 2017; 4: 49–58. https://doi.org/10.21548/4-2-2370

43. Madiraju AK, Erion DM, Rahimi Y, Zhang X-M, Braddock DT, Albright RA, et al. Metformin suppresses gluconeogenesis by inhibiting mitochondrial glycerophosphate dehydrogenase. Nature. 2014; 510: 542–546. https://doi.org/10.1038/nature13270 PMID: 24847880

44. Passalacqua TG, Torres FAE, Nogueira CT, de Almeida L, Del Cistia ML, dos Santos MB, et al. The 2′,4′-dihydroxychalcone could be explored to develop new inhibitors against the glycerol-3-phosphate dehydrogenase from *Leishmania* species. Bioorg Med Chem Lett. 2015; 25: 3564–3568. https://doi.org/10.1016/j.bmcl.2015.06.085 PMID: 26169126

45. Tomazela DM, Pupo MT, Passador EA., da Silva MF das G., Vieira PC, Fernandes JB, et al. Pyrano chalcones and a flavone from *Neoraputia magnifica* and their *Trypanosoma cruzi* glycosomal glyceraldehyde-3-phosphate dehydrogenase-inhibitory activities. Phytochemistry. 2000; 55: 643–651. https://doi.org/10.1016/s0031-9422(00)00248-x PMID: 11130676

46. Ou X, Ji C, Han X, Zhao X, Li X, Mao Y, et al. Crystal Structures of Human Glycerol 3-phosphate Dehydrogenase 1 (GPD1). J Mol Biol. 2006; 357: 858–869. https://doi.org/10.1016/j.jmb.2005.12.074 PMID: 16460752